Motor cortex stimulation for Parkinson's disease: a modelling study

2012 J. Neural Eng. 9 056005

(http://iopscience.iop.org/1741-2552/9/5/056005)

J. Neural Eng. **9** (2012) 056005 (12pp) doi:10.1088/1741-2560/9/5/056005

Motor cortex stimulation for Parkinson's disease: a modelling study

Daphne G M Zwartjes[1], Tjitske Heida[1], Hans K P Feirabend[2], Marcus L F Janssen[3,4], Veerle Visser-Vandewalle[5], Hubert C F Martens[6] and Peter H Veltink[1]

[1] MIRA Institute for Biomedical Engineering and Technical Medicine, Biomedical Signals and Systems Group, University of Twente, Enschede, The Netherlands
[2] Department of Anatomy & Embryology, Leiden University Medical Center, The Netherlands
[3] Department of Neuroscience, Maastricht University Medical Center, Maastricht, The Netherlands
[4] European Graduate School of Neuroscience (EURON), Maastricht, The Netherlands
[5] Department of Neurosurgery, Maastricht University Medical Center, Maastricht, The Netherlands
[6] Sapiens—Steering Brain Stimulation, Eindhoven, The Netherlands

E-mail: d.g.m.zwartjes@utwente.nl

Received 24 May 2012
Accepted for publication 19 July 2012
Published 10 August 2012
Online at stacks.iop.org/JNE/9/056005

Abstract
Chronic motor cortex stimulation (MCS) is currently being investigated as a treatment method for Parkinson's disease (PD). Unfortunately, the underlying mechanisms of this treatment are unclear and there are many uncertainties regarding the most effective stimulation parameters and electrode configuration. In this paper, we present a MCS model with a 3D representation of several axonal populations. The model predicts that the activation of either the basket cell or pyramidal tract (PT) type axons is involved in the clinical effect of MCS. We propose stimulation protocols selectively targeting one of these two axon types. To selectively target the basket cell axons, our simulations suggest using either cathodal or bipolar stimulation with the electrode strip placed perpendicular rather than parallel to the gyrus. Furthermore, selectivity can be increased by using multiple cathodes. PT type axons can be selectively targeted with anodal stimulation using electrodes with large contact sizes. Placing the electrode epidurally is advisable over subdural placement. These selective protocols, when practically implemented, can be used to further test which axon type should be activated for clinically effective MCS and can subsequently be applied to optimize treatment. In conclusion, this paper increases insight into the neuronal population involved in the clinical effect of MCS on PD and proposes strategies to improve this therapy.

(Some figures may appear in colour only in the online journal)

1. Introduction

Stimulation of the brain is increasingly used to treat Parkinson's disease (PD) and stimulation of the basal ganglia, deep brain stimulation (DBS), has become a widely accepted therapy for PD [1]. Chronic motor cortex stimulation (MCS) is a less invasive therapy, which was initially used for the treatment of chronic pain [2], but has now also been studied as a PD treatment, especially for patients who are not eligible for DBS or refuse this treatment [3, 4].

From a review of the literature and their own clinical data, Cioni *et al* [5] conclude that MCS may relieve all three main symptoms of PD (akinesia, rigidity, tremor), but results vary widely. Currently, MCS protocols for PD comprise either cathodal or bipolar stimulation [3–12]. There are, however, many uncertainties about the most effective stimulation parameters and electrode configuration. It is, for

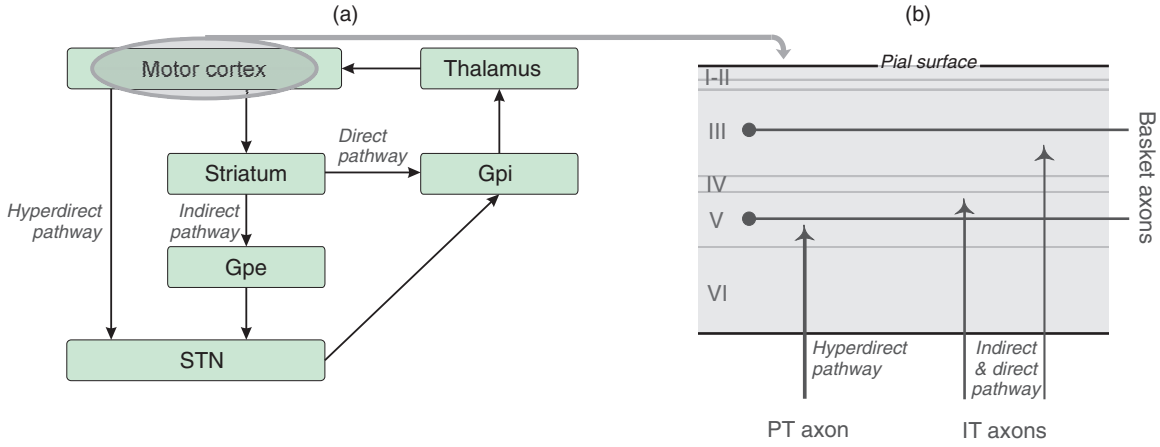

Figure 1. (a) The neuronal pathways from the cortex through the basal ganglia and thalamus back to the cortex. (b) A schematic representation of the axonal populations that have been suggested to play a role in the mechanisms of MCS for PD treatment: basket cell axons, which have inhibitory properties, are mainly located in layer III and V; PT type pyramidal axons, being excitatory and composing the hyperdirect pathway, originate from deep layer V [34]; IT type pyramidal axons, which are also excitatory and compose the direct and indirect pathway. Their somas are located in layer III, superficial and deep layer V [34] (those located in deep layer V are not considered, since their relatively small diameter makes them less excitable than PT type axons at similar locations).

example, not known whether subdural or epidural stimulation should be used [10–12] and which electrode orientation relative to the gyrus is optimal [4, 7, 10–13].

Since the mechanisms of MCS in the treatment of PD are not clear, information on how to optimize treatment is lacking. Several theories exist about the neuronal populations that are involved: (1) the involvement of the axons projecting to the hyperdirect pathway from the cortex to the subthalamic nucleus (STN) through which STN activity can be modulated (figure 1(a)) [3]. In cats, it has been shown that these axonal projections originate from the pyramidal tract (PT) type cells [14] (figure 1(b)), but this has not been studied in rats and monkeys yet [15]. (2) The axons projecting to the direct and indirect pathway (figure 1(a)) can also modulate basal ganglia activity [3, 4, 7, 13]. These pathways presumably originate from intratelecenphalic (IT) type pyramidal cells in the motor cortex [15, 16] and project to the striatum, or more particularly the lateral putamen [17], and then to the STN (figure 1(b)). (3) The involvement of the inhibitory axonal population [7, 12, 13, 18], i.e. the basket cells, which have long axons running parallel to the pial surface [19] (figure 1(b)). As the basket cells have multiple synaptic contacts on the pyramidal neurons [19], they can strongly inhibit this population and thereby modulate the cortico-basal ganglia loops. Additional networks in the cortex are formed by excitatory projections from the pyramidal neurons to the basket cells and other pyramidal neurons in different cortical layers [19]. Based on these theories, activation of three axonal populations has been suggested to play a role in MCS treatment for PD, namely basket cell axons, PT and IT type pyramidal axons.

To optimize treatment, it is important to know which axonal population is primarily involved in the clinical effect of MCS on PD. We propose a modelling approach using a finite element volume conduction model in combination with an axon model, similar to previously developed models for MCS [20–25] and DBS [26–29]. We extended previous MCS models by: considering axons with different orientations and at different depths in the grey matter (figure 1(b)); including new anatomical data on the diameters of the myelinated fibre populations [30]; using realistic models of PT and IT type pyramidal axons including axon collaterals [19, 31]; modelling axons in 3D space.

The aim is to determine which axonal populations are activated during clinically effective MCS treatment for PD using this computational model. Secondly, we will employ the model to determine protocols that selectively target these populations.

Although this paper is aimed at chronic MCS for PD, the outcome can also be useful for other applications, such as MCS for pain and stroke treatment and acute MCS to target the STN or GPi motor regions during DBS surgery [32, 33].

2. Methods

2.1. Volume conduction model

A 3D finite element volume conduction model of the MC including a current controlled stimulation electrode was developed using COMSOL Multiphysics (v3.4, COMSOL, Inc., Burlington, MA, USA). In addition, an axon model was developed in Matlab (MathWorks, Natick, MA, USA), using a finite impedance single cable model, which was virtually positioned in the MC.

The modelled MC geometry included the scalp, skull, dura mater, cerebrospinal fluid, grey matter and white matter (figure 2, table 1). Since quasi-static conditions can be assumed [35], the electrical potential field was calculated by solving Poisson's equation. Boundary conditions were based on a realistic head model [36], since Grant and Lowery showed that it is inadequate to use a simple cubic block grounded on the exterior boundaries for the representation of distant tissue. They propose a realistic model with electric insulation at the

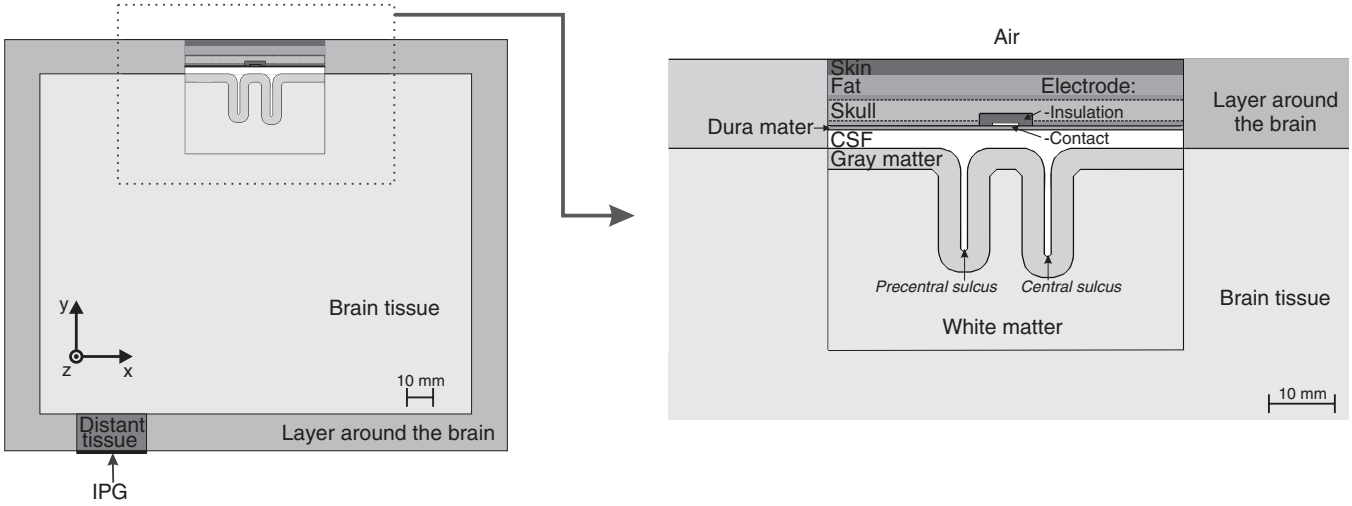

Figure 2. The finite element volume conduction model of the motor cortex with surrounding structures during epidural stimulation when the case of the IPG is used as a reference. On the left, the entire model, which is derived from a realistic head model, is shown. The area around the electrode, encompassed by dashed lines, is shown in more detail on the right. The layer around the brain represents the scalp, skull, dura mater and cerebro spinal fluid. The distant tissue represents the tissue in between the brain and clavicle, where the IPG is located. The entire model has the following dimensions: 192.1 × 157.1 × 167.1 mm.

Table 1. Parameters volume conduction model.

Geometry	dimensions (mm)	Conductivity (S m^{-1})
Skin	$y = 2.4$ [38]	0.00087 [39]
Fat	$y = 3.1$ [38]	0.042 [39]
Skull inner layer	$y = 3$ [37]	0.076 [39]
Skull outer layers	$y = 0.8$ and $y = 0.8$ [37]	0.02 [39]
Dura mater	0.36 [18]	0.055
Electrode insulation	$xyz = 8 \times 1.8 \times 44$	0.0001 [21]
Electrode contact	diameter = 2.3 or 4; height = 0.4	$6 \cdot 10^7$
Cerebrospinal fluid	$y = 3.1$ [21]	1.6 [40]
Grey matter	$y = 3.7$ [21]	0.36 [21]
Precentral gyrus	$x = 11.7$ [21]	
Central sulcus	$xy = 2.3 \times 16.4$ [21]	
Precentral sulcus	$xy = 2.7 \times 15.6$ [21]	
White matter	$xyz = 54 \times 30.4 \times 50$	$x = 0.083$; $y = 0.6$; $z = 0.083$ [21]
Layer around the brain	$xyz = 192.1 \times 157.1 \times 167.1$	0.0004
Distant tissue	$xyz = 40 \times 13.56 \times 40$	0.048
Brain tissue	$xyz = 165 \times 130 \times 140$	0.27 [41]

exterior boundaries and a ground located at the approximate location of the reference electrode. As only relative voltage values are of concern for the cable models of the axon, the reference electrode was set to 0 V. Their head model has an ellipsoid shape and incorporates a two-layered representation of the scalp, a three-layered representation of the skull and the cerebrospinal fluid. We replicated this model and added the dura mater. Subsequently, the realistic model was simplified by converting the ellipsoid shape of the head to a block (figure 2). Furthermore, outside the area of interest, which is an area of about 30 mm around the electrode, the different shells representing the scalp, skull, dura mater and cerebrospinal fluid were converted to one layer. The effective conductivity of this layer was chosen such that the electric potential (in the grey matter right beneath the stimulation electrode) and impedance in the simplified model differed less than 2% from the electric potential and impedance in the realistic version. The boundary conditions in the realistic model and simplified model were similar, i.e. exterior boundaries were electrically insulated and the reference electrode was set to 0 V. During monopolar stimulation, the reference electrode was located on the case of the implantable pulse generator (IPG; figure 2) [3, 4, 6, 8–11]. During bipolar stimulation, one of the remaining electrode contacts was used as a reference. Like Manola *et al* [21], we set the conductance of the dura mater to a value that gives an impedance matching to the mean empirical value of ∼1000 Ω during bipolar stimulation. This resulted in a conductance of 0.055 S m^{-1}, which is in between the values of 0.065 S m^{-1} proposed by Manola *et al* [21] and 0.03 S m^{-1} used by Struijk *et al* [37]. The conductance of the 'distant tissue' representing tissue in between the brain and clavicle, where the case of the IPG is located, was determined by matching the model impedance during monopolar stimulation to the mean empirical value of ∼750 Ω [21]. The finite element model was $19 \times 16 \times 17$ cm^3 and it was solved for 9.2×10^4 tetrahedral elements using a linear solver, conjugate gradients, with preconditioning of an algebraic multigrid solver. The finest mesh is located in the electrode contact where the mesh

Table 2. Parameters axon model.

Parameter	Value
Neuron resting potential	−0.084 V [46]
Intracellular resistivity	0.4 Ωm [47]
Membrane capacitance	0.028 F m^{-2} [48]
Myelin membrane capacitance	0.0005 F m^{-2} [49]
Myelin membrane conductance	5 S m^{-2} [49]

elements had an average volume of 0.041 mm^3. The mesh element volume increased to an average of 412 mm^3 in the roughest meshed structure; the brain tissue. Increasing the overall resolution approximately twofold resulted in a less than 2% difference of the electric potential in the grey matter beneath the stimulation electrode.

2.2. Axon model

Instead of an entire neuron, only the axon was modelled since axons are the key neuronal components responding to MCS, i.e. the component that primarily causes the output activity of the stimulated structure [20, 42, 43]. The axon was modelled as a single cable model with the myelin having a finite resistance and capacitance; details can be found in [44, 45]. The parameters applied in the axon model are listed in table 2. Details on the ion channel and leakage conductances are presented in the appendix.

The following boundary conditions were used in the axon model: at the start and end of the axons, the next 'virtual' compartment was assumed to have the same membrane potential value as the boundary compartment. This ensures that no action potentials will be generated by boundary effects. Activation of an axon was defined when the membrane potential of one of the nodes was raised by 70 mV from the rest potential.

Different types of axons are located in the motor cortex. Since we are interested in those that might be involved in the clinical effect of MCS on PD, we modelled the basket cell, PT and IT type axons (figure 1). We assume that the direct and indirect pathways are (solely) innervated by IT type axons. Although one study argues that the PT type axons provide the main input to the direct pathway [50], recent work [15, 16] indicates that the IT type axons are the most important input. The inhibitory double bouquet cells and chandelier cells, which have axons oriented perpendicular to the pial surface, were not modelled as their axons run alongside pyramidal axons, which typically have a larger diameter [51] and are, therefore, more excitable.

The inhibitory axonal population was represented by basket cell axons, which were modelled as long axons running parallel to the pial surface at depths of 1950 μm and 850 μm from the pial surface, being halfway the fifth and the third layer, respectively ([19]; figure 3, red and orange). These axons were placed in 91 *xy*-planes spaced 0.33 mm apart in *z*-direction: −15 to +15 mm from the middle in between the two electrode contacts. Thereby, 3D populations of 91 basket cell axons in both the fifth and third layer were obtained. The pyramidal axons (the PT and IT type axons) were placed such that the soma (which was not modelled) would lie at distances of 2125, 1775 and 1125 μm from the pial surface. These depths correspond to the PT axon at three-fourth of layer V, and the IT axons at one-fourth of layer V and three-fourth of layer III, respectively. Furthermore, they were placed in the *xy*-plane in three different ways (figure 3): (1) a vertical axon right beneath the stimulation electrode on the crown of the gyrus (blue); (2) a diagonal axon running through the lip (purple); and (3) a horizontal axon running through the sulcus bank (green) [24]. They were also placed in *z*-direction from −15 to +15 mm, using 31 *xy*-planes spaced 1 mm apart, obtaining a population of 93 PT type axons in layer V, 93 IT type axons in both layer III and V. The pyramidal axons were represented by a main axon and an axon collateral [19, 31] (figure 3). Two types of axon collaterals were used, both lying parallel to the pial surface but oriented differently with respect to the medial–lateral and anterior–posterior axis (figure 3). Each pyramidal axon model was modelled using collateral type 1 or 2 and a 50% presence of both types was assumed. It was checked that the pyramidal axon model produced results consistent with several experimental studies [18, 32, 52].

The diameters of the basket cell axon models were retrieved from Feirabend *et al* [30]. They assessed the diameter of the myelinated fibre population, which they define as the thickness of the axon including the myelin sheets, in the human motor cortex. The axon diameter in our model is defined similarly. Only fibres with a diameter above 5 μm were considered by Feirabend *et al* because thinner fibres are less interesting since they become increasingly difficult to activate. They distinguished diameters between differently oriented axons and between axons at different depths in the grey matter. As basket cell axons are mainly located in layer III and V [19], we used the axon diameters found at depths corresponding to the middle of both layers: the basket cell axon has an average diameter of 5.4 μm in layer III and 5.7 μm in layer V.

The diameters of the pyramidal axons were derived from average diameters measured in human and the ratio between the axon diameters of different neuron types found in rat. The average diameter of perpendicularly oriented axons in the human motor cortex is 7.1 μm [30]. We differentiated different neuron types and neurons at different depths, by using ratios of soma sizes found in the rat motor cortex [34], which were converted to axon diameters using the relation between axon and soma diameters [51]. The following diameters were used: 10.6, 5.1 and 5.7 μm for PT type axons in layer V and IT type axons in layer III and V, respectively. The axon collaterals of these perpendicular axons ran parallel to the pial surface. The diameters of these collaterals were based on the diameter-ratio between parallel and perpendicular axon diameters in human 0.85:1 [30]. This gave collateral diameters of 9.0, 4.5 and 4.8 μm for the PT type axons in layer V and IT type axons in layer III and V, respectively.

2.3. Simulations

The simulations consisted of two parts: defining which axonal populations are activated during clinically effective

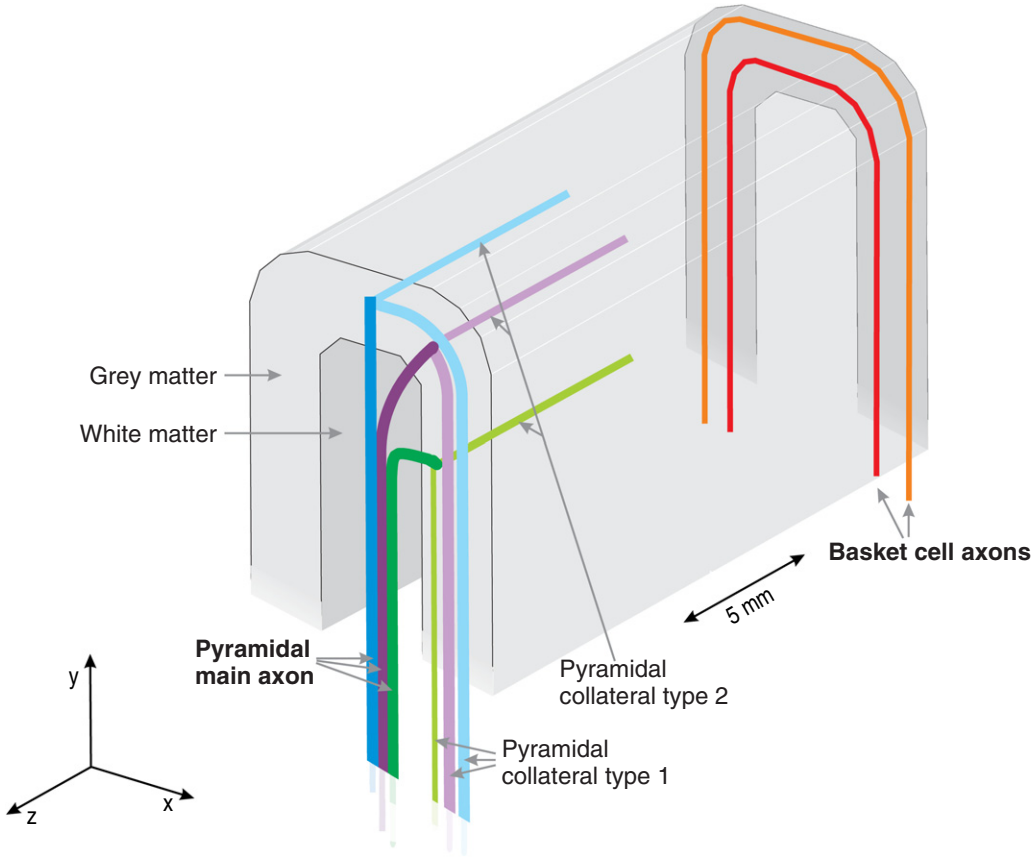

Figure 3. The motor cortex in which the basket cell axon, PT and IT type pyramidal axon models are shown: basket axons in layer III (orange) and layer V (red); pyramidal axons (blue, purple and green). The pyramidal axons in one layer of one type are shown. In reality there is the PT type in layer V and IT type in layer III and V. The different colours represent three orientations. The pyramidal axons are modelled using a main axon and axon collaterals type 1 and 2. For illustrative purposes, the three pyramidal axons with collaterals are shown with a small distance in between the collaterals type 1, but in reality they overlie one another. Only one *xy*-plane is shown for each axonal type, while multiple planes in *z*-direction were modelled.

MCS for PD; and proposing stimulation protocols to target these populations selectively. In both parts, the effect of the stimulation protocols was assessed by determining the activation threshold for each individual axon and subsequent computation of the activation fraction. The activation fraction is defined as the percentage of activated axons from the total amount of axons we modelled in our 3D population. Assuming that, within a volume of $8.2 \cdot 10^3$ mm^3 an equal number of each axon type exists, i.e. 91 basket cell axons in both layer III and V, 93 IT type axons in both layer III and V, and 93 PT type axons. Results were obtained within clinically relevant stimulation amplitudes, which are up to 8 V [7]. Considering impedances of 750 and 1000 Ω during monopolar and bipolar stimulation, respectively [21], this corresponds to 10.7 and 8 mA.

The first part of the simulations assess which neuronal populations are activated during clinically effective MCS treatment. This will be done by studying the effects of cortical stimulation on the earlier proposed axonal populations: the basket cell, PT and IT type axons. The clinically effective stimulation protocols are epidural cathodal and bipolar stimulation (table 3). The effect of monopolar anodal stimulation has not been studied on humans as this is not possible due to the design of the present IPGs [12].

In the second part, we looked for selective MCS protocols by varying the position and orientation of the strip, the contact size and the distance between the contacts, the stimulation type, i.e. anodal/cathodal/bipolar, and the number of cathodes (table 3).

3. Results

3.1. Axonal populations activated during clinically effective MCS for PD

The activation fractions during clinically effective stimulation protocols (table 3, first row) are shown in figures 4(a) and (b). The activation fraction of the basket cell axons was largest during cathodal stimulation, but the PT type pyramidal axons were also activated. The IT type pyramidal axons were activated at a threshold of 13.5 mA, which is beyond the clinical range of stimulation amplitudes used during MCS. During bipolar stimulation, all axon types were activated, but the activation fractions of basket cell and PT type axons were larger than those of IT type axons. Furthermore, a larger fraction of the more superficially located basket cells in layer III were activated than those in layer V in both stimulation protocols.

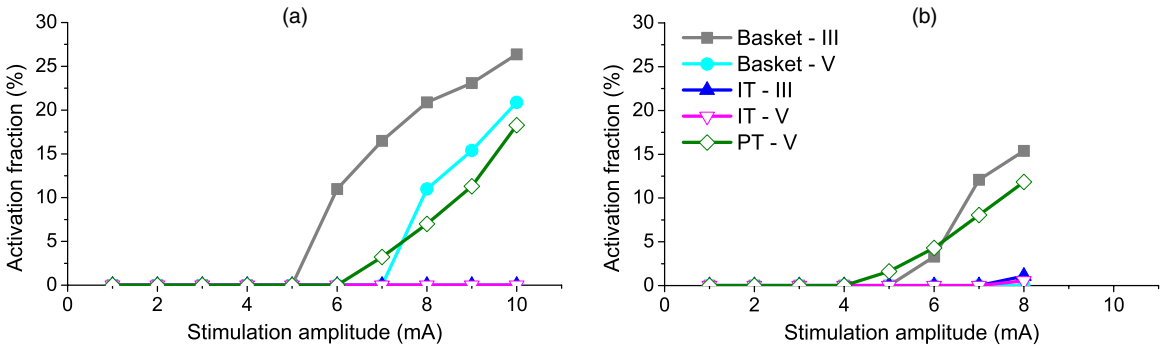

Figure 4. The activation fractions of different axonal populations that are believed to be involved in the mechanisms of MCS on PD. The clinically used stimulation protocols, epidural cathodal (a) and bipolar (b) stimulation, were modelled.

Table 3. MCS protocols.

Protocols	Position	Strip orientation[a]	D (mm)	I (mm)	Electrode configurations[b]
Clinical	Epidural	Parallel	4	10.2	- ; +-
Variations					
1	Epidural	Parallel	4	10.2	+
2	Subdural	Parallel	4	10.2	+
3	Epidural	Perpendicular	4	10.2	+
4	Epidural	Parallel	2; 6	10.2	+
5	Subdural	Parallel	4	10.2	-
6	Epidural	Perpendicular	4	10.2	-
7	Epidural	Parallel	2; 6	10.2	-
8	Epidural	Parallel	4	10.2	-- ; -o- ; --- ; +o- ; +--
9	Epidural	Parallel	4	5.1; 15.3	+-

The first row shows clinically used MCS protocols [3–12]. The remaining rows show the variations on the clinical protocols, which are assessed to find selective stimulation protocols. Each variation is numbered. The change relative to the clinical protocols is shaded.
[a]Strip orientation relatively to the gyrus.
[b]Electrode configurations: '+' is anode, '−' is cathode and 'o' is not active. When multiple cathodes were used, the current was divided between the contacts.

To get more insight into how the activation spreads in the cortex, the spreading of the basket cell axon activation is depicted in figure 5. This distribution is slightly asymmetrical, because of the location of the reference electrode which influences the gradient of the potential field.

The activation of the axons was initiated at different nodes during different stimulation protocols. The following results were found for axons activated within the clinically used range of stimulation amplitudes. During anodal stimulation, excitation of the vertical pyramidal axons (figure 3, blue) started close to the boundary of the grey and white matter on the main axon. During cathodal stimulation, excitation of the vertical pyramidal axons (figure 3, blue) initiated at the axon collaterals close to the main axon, while the diagonal and horizontal pyramidal axons (figure 3, purple and green) were activated first at nodes located in the bending part of the main axon. During cathodal stimulation, basket cell axons (figure 3, orange and red) were activated first on the node in the horizontal part of the axon closest to the stimulation electrode. When considering bipolar stimulation, the locations of activation on the axons beneath the anode were similar to monopolar anodal stimulation, and beneath the cathode similar to monopolar cathodal stimulation.

3.2. Establishing more selective stimulation protocols

An extensive number of protocols were assessed in order to achieve more selective stimulation. The results of our model described above indicate that the basket cell and PT type pyramidal axonal populations are excited in all clinically effective MCS protocols, while IT type pyramidal axons are not activated in all effective protocols. Therefore, we assume that the activation of IT type pyramidal axons is not involved in the clinical effect of MCS on PD and further assess selective stimulation of basket cell axons and PT type pyramidal axons.

First, we assessed the two clinically applied protocols and varied the electrode configuration with an anode (table 3—variation 1; figure 6). It is shown that cathodal stimulation most

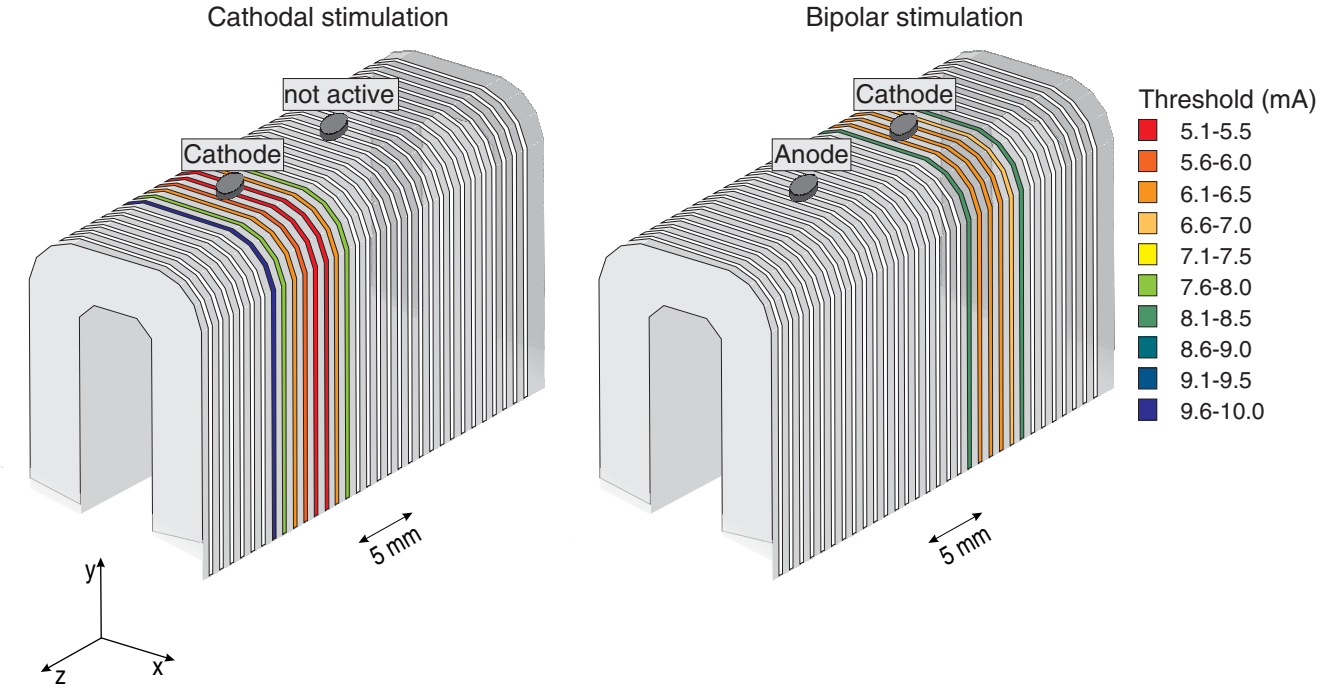

Figure 5. The spreading of the activation of the basket cell axons in layer III during cathodal and bipolar epidural stimulation. Note that for illustrative reasons the basket cell axons are depicted on the surface of the gyrus, while they are modelled at a depth corresponding to the middle of the third cortical layer.

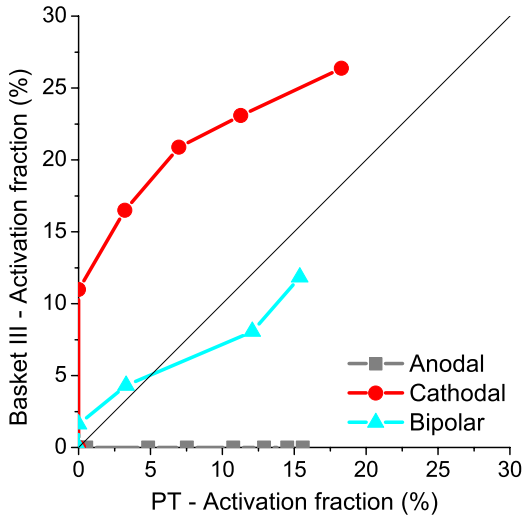

Figure 6. The two clinically applied stimulation protocols (table 3) and a variation in the electrode configuration, i.e. monopolar anodal stimulation (variation 1). Each point represents the activation fraction for a certain stimulation amplitude, which increases from 1 to 10 mA, in steps of 1 mA. Basket cell axons are most selectively activated during cathodal stimulation, while anodal stimulation selectively targets the PT type pyramidal axons.

selectively activates basket cell axons, while PT type axons are selectively targeted using anodal stimulation. Using these electrode configurations as a starting point, more selective stimulation protocols will be developed.

3.2.1. Basket cell axons. The cathodal stimulation protocol most selectively stimulated basket cell axons (figure 6). As IT type axons were not activated at all during this stimulation protocol (figure 4(a)), the selectivity of basket cell axons against PT type axons was investigated further. Variations 5–9 (table 3) were assessed.

Selective stimulation of basket cell axons can be improved by using multiple cathodes (variation 5; figure 7(a)). The optimal location and number of cathodes depended on the required basket cell activation fraction. For higher fractions, multiple cathodes are preferable, while for lower fractions a single cathode or two separate cathodes offer the best selectivity. A second approach to stimulate the basket cell axons more selectively was by using bipolar stimulation while placing the electrode strip perpendicular to the gyrus over the central sulcus with the cathode on top of the gyrus (variation 8). Compared to the cathodal stimulation protocol, the basket cell axons were activated more selectively relatively to the PT type axons (figure 7(b)). Bipolar stimulation with the contacts placed closer to each other or further apart (variation 6) did not give a higher selective activation of the basket cell axons. The electrode location (epidural/subdural; variation 7) and contact diameter (variation 9) had little influence on selectivity of basket cell axons relatively to the PT population.

3.2.2. PT type pyramidal axons. Figure 6 shows that anodal stimulation (variation 1) offers the highest selectivity for PT type pyramidal axons activation. As basket cell axons are not activated at all within the clinically relevant stimulation amplitudes during anodal stimulation, the selectivity of PT type against IT type pyramidal axons is explored further. Variations 1–4 and 6 were assessed. Increased selectivity of PT type axon stimulation can be achieved by increasing the contact size (variation 4; figure 8(a)). Using subdural rather

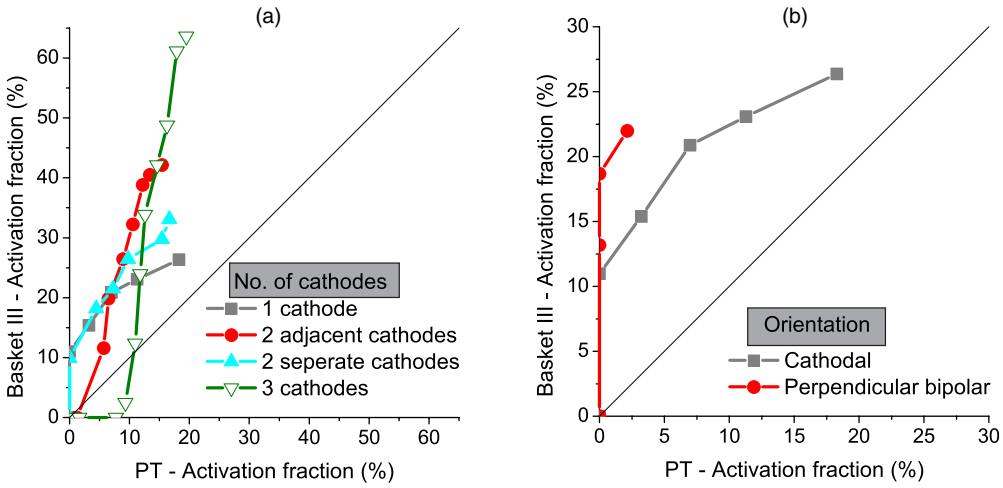

Figure 7. The following variations on the cathodal stimulation protocol provided more selective stimulation of the basket cell axons relatively to the PT type pyramidal axons. Each point represents the activation fraction for a certain stimulation amplitude, which increases from 1 to 10 mA, in steps of 1 mA. (a) The activation fraction for a varying number of epidurally placed cathodes (variation 5). For basket cell axon activation fractions up to ∼20%, one cathode or two separate cathodes offered the highest selectivity. For larger activation fractions, two adjacent cathodes resulted in increased selectivity, and for fractions above 41% three cathodes was the best choice. (b) The perpendicular bipolar protocol with the cathode placed over the gyrus (variation 8) provided more selective stimulation of basket cell axons than the cathodal stimulation protocol.

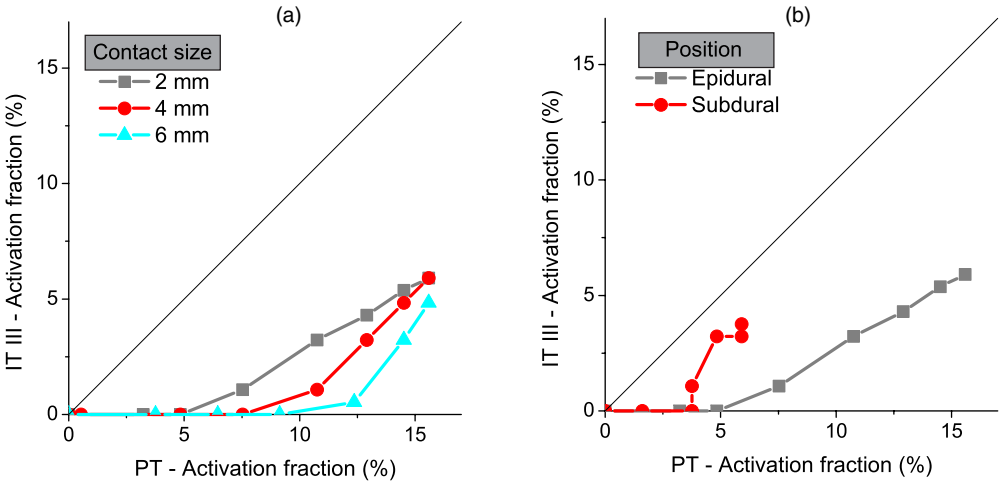

Figure 8. (a) The selectivity of the activation of PT type against IT type pyramidal axons during anodal stimulation increased with a larger contact size (variation 4). Each point represents the activation fraction for a certain stimulation amplitude, which increases from 1 to 10 mA, in steps of 1 mA. (b) PT type axons were activated more selectively during epidural stimulation than during subdural stimulation. The activation fraction for increasing stimulation amplitudes from 0.1 to 1 mA, in steps of 0.1 mA, are shown.

than epidural stimulation resulted in a lower selectivity toward PT type axons (variation 2; figure 8(b)). This selectivity was also decreased when using bipolar stimulation (variation 3) with the anode on top of the gyrus and the strip placed perpendicular to the gyrus over the sulcus and when using bipolar stimulation with the contacts spaced closer to each other or further away (variation 6).

4. Discussion

4.1. Axonal population responsible for clinically effective MCS on PD

We examined the activation of several axonal populations in order to identify the populations activated during clinically effective MCS treatment for PD. We found that IT type pyramidal axons were not activated during all clinically effective stimulation protocols, while both basket cell axons and PT type pyramidal axons were activated. This suggests that it is unlikely that the activation of IT type axons is responsible for the clinical effect MCS has on PD. Our model predicts that either the activation of basket cell axons or PT type pyramidal axon is involved in this clinical effect.

Activation of the basket cell axons supports the theory that the inhibitory axonal population plays an important role in the clinical effect of MCS on PD [7, 12, 13, 18]. However, since the pyramidal neurons that innervate the hyperdirect, direct and indirect pathways are inhibited by the basket cells, theories suggesting the involvement of these pathways are also likely true [3, 4, 7, 13]. These network properties are important

as chronic MCS is performed by applying a continuous train of pulses instead of just a single pulse as in our model. The result of train stimulation is a cumulative sum of the facilitating and inhibitory effects; thus, the effect of stimulation trains may depend on whether facilitation or inhibition dominates the response to single stimuli [18]. The main hypothesis on the mechanisms of DBS concerns prevention of the transmission of the pathologic network activity generated in the cortico-basal-ganglia-thalamo-cortical loop [53]. Likewise, the basket cells have inhibitory properties and can thereby reduce the loop-gain in the motor cortex, which could prevent transmission of the pathological activity in these loops.

Activation of the PT type pyramidal axons agrees with theories suggesting modulation of the hyperdirect pathway to play a role in the mechanisms of MCS [3], but as these axons innervate other pyramidal axons, excitation of the direct and indirect pathways could also explain the clinical effect [4, 7, 13].

4.2. Establishing more selective stimulation protocols

Since our model predicts that either the basket cell axons or the PT type pyramidal axons are highly likely candidates for the clinical effect, activation of these axonal populations with a higher selectivity was assessed. Selective targeting of the population involved in the clinical effect could improve the effect of the treatment.

Based on the modelling results, cathodal epidural stimulation, often used to treat PD, is the protocol that most selectively targets the basket cell axons. The following protocols can increase this selectivity even further: the use of multiple cathodes either adjacent or with an inactive contact in between; applying bipolar stimulation rather than cathodal stimulation with the electrode strip placed perpendicular to the gyrus and the cathode overlying the gyrus. The contact size of the electrode contacts and the use of epidural rather than subdural stimulation did not influence selectivity toward basket cell axons during cathodal stimulation.

According to our model, selective stimulation of PT type pyramidal axons can be achieved by anodal epidural stimulation using electrodes with large contact sizes. Selective stimulation of the PT type axons was reduced when using subdural stimulation and bipolar stimulation with the strip oriented parallel as well as perpendicular to the gyrus.

In the future, these new protocols should be tested experimentally with evaluation of the effect on motor symptoms using clinical rating scales [54] and objective movement measurements [55]. This could help to confine which axonal population, i.e. basket cell axons or PT type pyramidal axons, should be activated in order to achieve clinically effective stimulation for the treatment of PD. The selective protocols could offer means to improve this treatment.

4.3. Comparison to previous modelling studies

Assessing the location at which the axon was excited, we found that during anodal stimulation excitation generally started at a node close to the grey and white matter boundary. This is in agreement with earlier modelling studies [24, 25]. Like Salvador *et al* [31], we found that during cathodal stimulation, the action potential was generated at the axon collateral in the vertical pyramidal axon (figure 3, blue). They indicated that with large diameter differences between the main and collateral axon, the action potential did not propagate from the collateral to the main axon. However when considering diameter differences consistent with our model, they did see propagation to the main axon, which is similar to our findings. In addition, they also found activation to be started on a node at the bend of the main axon in the diagonal and horizontal pyramidal axons (figure 3, purple and green). Furthermore, during cathodal stimulation the basket cell axons were activated in the nodes closest to the electrode at the horizontal part of the main axon, which is similar to Manola's findings [24]. During bipolar stimulation, axons beneath the anode and cathode were activated at similar locations compared to monopolar stimulation. This is in agreement with the findings of Holsheimer *et al* [56], who argued that bipolar stimulation with the electrodes at least 10 mm apart is actually bifocal.

Our model shows that anodal stimulation favours activation of axons running perpendicular to the pial surface, i.e. pyramidal axons (figure 6), which is in agreement with a previous model study on MCS for pain [24]. Cathodal stimulation selectively activates basket cell axons, which run parallel to the pial. This is also in agreement with the study of Manola *et al* [24]. In contrast, our results also show activation of the vertical pyramidal axons (figure 3, blue), which were not activated in Manola's study. This is caused by the inclusion of axon collaterals in the pyramidal axon model.

4.4. Model limitations

In our model, we simulated single pulse stimulation. As the clinical application of MCS encompasses high frequency chronic stimulation, network properties are involved [18]. The final effect of the stimulation depends on parameters such as the number of synaptic contacts and their strengths, as well as the axon density. These parameters are, except for certain axon density parameters [30], not yet sufficiently available. Therefore, we looked at activation fractions of different axonal populations relatively to one another. Second, we used a fixed CSF-layer thickness, while the thickness depends on the brain location and is different per person. This will probably influence model outcomes [21] and it could therefore be included in patient specific models in the future. Third, the axon was modelled without a soma and dendrites, while both influence the axon boundary node. This may have introduced a small difference in the results, especially in the pyramidal axons which have somas close to the electrode contact. Fourth, although the diameters were for a large part based on human data, the ratios between the PT and IT type axon diameters were based on rat data, as no human data was available on this. Finally, the basket cell axons were modelled running parallel to the pial surface in the *xy*-plane, while they also run in *z*-direction (figure 3). This likely has the largest influence on the results of bipolar stimulation parallel to the gyrus, which

will probably excite basket cell axons running in z-direction relatively more easily. This would provide better selective stimulation of basket cell axons than anticipated in our current model, which is in favour of the hypothesis that these axon type is involved in clinically effective stimulation.

5. Conclusions

Our computational model predicts that the clinical effect of MCS in the treatment of PD is related to the activation of either the inhibitory basket cell axonal population or the excitatory PT type pyramidal axons. Selective stimulation of the basket cell axonal population can be achieved using cathodal, rather than anodal stimulation. When bipolar stimulation is applied, the electrode strip is preferably placed over the sulcus perpendicular to the gyrus. Furthermore, selective stimulation of the basket cell axons can be increased by the use of multiple cathodes. PT type pyramidal axons can be selectively targeted using anodal stimulation with electrodes having large contact sizes. Epidural stimulation is advisable over subdural stimulation. To further confine which population is involved in the clinical effect of MCS, protocols selectively targeting one of both axonal populations can be tested for their effect on PD. Such selective stimulation protocols could also improve MCS for PD. In conclusion, this study provides more insight into the neuronal population involved in the clinical effect of chronic MCS on PD and proposes strategies to improve this therapy.

Acknowledgments

The authors would like to thank S Canavero for the helpful discussions. The authors gratefully acknowledge the support of the BrainGain in Smart Mix Programme of the Netherlands Ministry of Economic Affairs and the Netherlands Ministry of Education, Culture and Science.

Appendix.

The axon model [46] at 37 °C.

Gating variables, with the gating coefficients α and β in s-1 and the membrane potential at the node, V_n, in V.

$$\alpha_m = \frac{7.1 * 10^6 (V_n + 0.0184)}{1 - \mathrm{e}^{\frac{-0.0184 - V_n}{0.0103}}}$$

$$\beta_m = \frac{3.3 * 10^5 (-0.0227 - V_n)}{1 - \mathrm{e}^{\frac{V_n + 0.0227}{0.0092}}}$$

$$\alpha_h = \frac{2.1 * 10^5 (-0.111 - V_n)}{1 - \mathrm{e}^{\frac{V_n - 0.111}{0.011}}}$$

$$\beta_h = \frac{1.4 * 10^4}{1 + \mathrm{e}^{\frac{-0.0288 - V_n}{0.0134}}}$$

$$\alpha_n = \frac{5.2 * 10^4 (V_n + 0.0932)}{1 - \mathrm{e}^{\frac{-0.0932 - V_n}{0.0011}}}$$

$$\beta_n = \frac{9.2 * 10^4 (-0.076 - V_n)}{1 - \mathrm{e}^{\frac{V_n + 0.076}{0.0105}}}$$

$$\alpha_s = \frac{7.9 * 10^3 (V_n + 0.0125)}{1 - \mathrm{e}^{\frac{-0.0125 - V_n}{0.0236}}}$$

$$\beta_s = \frac{4.8 * 10^3 (-0.0801 - V_n)}{1 - \mathrm{e}^{\frac{V_n + 0.0801}{0.0218}}}$$

$$\frac{\mathrm{d}m}{\mathrm{d}t} = \alpha_m (1 - m) - \beta_m m$$

$$\frac{\mathrm{d}h}{\mathrm{d}t} = \alpha_h (1 - h) - \beta_h h$$

$$\frac{\mathrm{d}n}{\mathrm{d}t} = \alpha_n (1 - n) - \beta_n n$$

$$\frac{\mathrm{d}s}{\mathrm{d}t} = \alpha_s (1 - s) - \beta_s s.$$

The ionic currents and leakage are in A m^{-2}.

Sodium current

$$I_{Na} = m^3 * h * J$$

$$J = \frac{P_{Na} z^2 F^2 V_n}{RT} \frac{Na_i - Na_o \mathrm{e}^{-\frac{zFV_n}{RT}}}{1 - \mathrm{e}^{-\frac{zFV_n}{RT}}}$$

Fast potassium current

$$I_{Kf} = n^4 g_{Kf} (V_n - V_K)$$

Slow potassium current

$$I_{Ks} = s g_{Ks} (V_n - V_K)$$

Leakage current

$$I_L = g_L (V_n - V_L)$$

Sodium permeability, $P_{\mathrm{Na}} = 7.04 \cdot 10^{-5}$ m s^{-1}
Sodium ion valency, $z = 1$
Faraday's constant, $F = 96485$ C mol^{-1}
Gas constant, $R = 8.3144$ J K*mol^{-1}
Temperature, $T = 310$ K
Intracellular Na concentration, $\mathrm{Na}_i = 18$ mM
Extracellular Na concentration, $\mathrm{Na}_o = 154$ mM
Potassium equilibrium potential, $V_k = -0.0887$ V
Leakage equilibrium potential, $V_L = -0.084$ V
Fast K conductance, $g_{\mathrm{Kf}} = 300$ S m^{-2}
Slow K conductance, $g_{\mathrm{Ks}} = 600$ S m^{-2}
Leak conductance, $g_L = 400$ S m^{-2}.

References

[1] Benabid A L 2003 Deep brain stimulation for Parkinson's disease *Curr. Opin. Neurobiol.* **13** 696–706
[2] Tsubokawa T, Katayama Y, Yamamoto T, Hirayama T and Koyama S 1991 Treatment of thalamic pain by chronic motor cortex stimulation *PACE-Pacing Clin. Electrophysiol.* **14** 131–4
[3] Pagni C A *et al* 2005 Extradural motor cortex stimulation (EMCS) for Parkinson's disease. History and first results by the study group of the Italian neurosurgical society *Acta Neurochir.* **S93** 113–9
[4] Cioni B 2007 Motor cortex stimulation for Parkinson's disease *Acta Neurochir.* **S97** 233–8
[5] Cioni B, Bentivoglio A, De Simone C, Fasano A, Piano C, Policicchio D, Perotti V and Meglio M 2009 *Invasive Cortical Stimulation for Parkinson's Disease and Movement Disordered* ed S Canavero (New York: Nova Science)

[6] Canavero S and Paolotti R 2000 Extradural motor cortex stimulation for advanced Parkinson's disease: case report *Mov. Disord.* **15** 169–71
[7] Meglio M and Cioni B 2009 *Textbook of Stereotactic and Functional Neurosurgery* vol 7 ed A M Lozano *et al* (Berlin: Springer) pp 1679–90
[8] Drouot X *et al* 2004 Functional recovery in a primate model of Parkinson's disease following motor cortex stimulation *Neuron* **44** 769–78
[9] Fasano A, Piano C, De Simone C, Cioni B, Di Giuda D, Zinno M, Daniele A, Meglio M, Giordano A and Bentivoglio A 2008 High frequency extradural motor cortex stimulation transiently improves axial symptoms in a patient with Parkinson's disease *Mov. Disord.* **23** 1916–9
[10] Arle J E, Apetauerova D, Zani J, Deletis D V, Penney D L, Hoit D, Gould C and Shils J L 2008 Motor cortex stimulation in patients with Parkinson disease: 12-month follow-up in 4 patients *J. Neurosurg.* **109** 133–9
[11] Gutierrez J C, Seijo F J, Alcarez Vega M A, Fernandez Gonzalez F, Lozano Aragoneses B and Blazquez M 2009 Therapeutic extradural cortical stimulation for Parkinson's disease: report of six cases and review of the literature *Clin. Neurol. Neurosurg.* **111** 703–7
[12] Arle J E and Shils J L 2008 Motor cortex stimulation for pain and movement disorders *Neurotherapeutics* **5** 37–49
[13] Cioni B, Meglio M, Perotti V, De Bonis P and Montano N 2007 Neurophysiological aspect of chronic motor cortex stimulation *Clin. Neurophysiol.* **37** 441–7
[14] Giuffrida R, Li Volsi G, Maugeri G and Percivalle V 1985 Influences of pyramidal tract on the subthalamic nucleus in the subthalamic nucleus of the cat *Neurosci. Lett.* **54** 231–5
[15] Mathai A and Smith S 2011 The corticostriatal and corticosubthalamic pathways: two entries, one target. So what? *Front. Syst. Neurosci.* **5** 64
[16] Ballion B, Mallet N, Bézard E, Lanciego J L and Gonon F 2008 Intratelencephalic corticostriatal neurons equally excite striatonigral and striatopallidal neurons and their discharge activity is selectively reduced in experimental parkinsonism *Eur. J. Neurosci.* **27** 2313–21
[17] Takada M, Tokuno H, Nambu A and Inase M 1998 Corticostriatal projections from the somatic motor areas of the frontal cortex in the macaque monkey: segregation versus overlap of input zones from the primary motor cortex, the supplementary motor area, and the premotor cortex *Exp. Brain Res.* **120** 114–28
[18] Hanajima R, Ashby P, Lang A E and Lozano A M 2002 Effects of acute stimulation through contacts placed on the motor cortex for chronic stimulation *Clin. Neurophysiol.* **113** 635–41
[19] Nieuwenhuys R 1994 The neocortex. An overview of its evolutionary development, structural organization and synaptology *Anat. Embryol.* **190** 307–37
[20] Manola L and Holsheimer J 2007 Motor cortex stimulation: role of computer modelling *Acta Neurochir.* **S97** 497–503
[21] Manola L, Roelofsen B H, Holsheimer J, Marani E and Geelen J A 2005 Modelling motor cortex stimulation for chronic pain control: electrical potential field, activating functions and responses of simple nerve fibre models *Med. Biol. Eng. Comput.* **43** 335–43
[22] Silva S, Basser P J and Miranda P C 2008 Elucidating the mechanisms and loci of neuronal excitation of transcranial magnetic stimulation using a finite element model of cortical sulcus *Clin. Neurophysiol.* **119** 2405–13
[23] Wongsarnpigoon A and Grill W M 2008 Computational modeling of epidural cortical stimulation *J. Neural Eng.* **5** 443–54
[24] Manola L, Holsheimer J, Veltink P H and Buitenweg J R 2007 Anodal vs cathodal stimulation of motor cortex: a modeling study *Clin. Neurophysiol.* **118** 464–74
[25] Wongsarnpigoon A and Grill W M 2012 Computer-based model of epidural motor cortex stimulation: effects of electrode position and geometry on activation of cortical neurons *Clin. Neurophysiol.* **123** 160–72
[26] McIntyre C C, Mori S, Sherman D L, Thakor N V and Vitek J L 2004 Electric field and stimulating influence generated by deep brain stimulation of the subthalamic nucleus *Clin. Neurophysiol.* **115** 589–95
[27] Sotiropoulos S N and Steinmetz P N 2007 Assessing the direct effects of deep brain stimulation using embedded axon models *J. Neural Eng.* **4** 107–19
[28] Butson C R and McIntyre C C 2008 Current steering to control the volume of tissue activated during deep brain stimulation *Brain Stimul.* **1** 7–15
[29] Frankemolle A M M, Wu J and Noecker A M 2010 Reversing cognitive-motor impairments in Parkinson's disease patients using a computational modelling approach to deep brain stimulation programming *Brain* **133** 746–61
[30] Feirabend H K P *et al* 2011 personal communication
[31] Salvador R, Silva S, Basser P J and Miranda P C 2011 Determining which mechanisms lead to activation in the motor cortex: a modeling study of transcranial magnetic stimulation using realistic stimulus waveforms and sulcal geometry *Clin. Neurophysiol.* **122** 748–58
[32] Janssen M L F, Zwartjes D G M, Temel Y, Van Kranen-Mastenbroek V, Duits A, Bour L J, Veltink P H, Heida T and Visser-Vandewalle V 2012 Subthalamic neuronal responses to cortical stimulation *Mov. Disord.* **27** 435–8
[33] Nishibayashi H, Ogura M, Kakishita K, Tanaka S, Tachibana Y, Nambu A, Kita H and Itakura T 2011 Cortically evoked responses of human pallidal neurons recorded during stereotactic surgery *Mov. Disord.* **26** 469–76
[34] Reiner A, Jiao Y, Del Mar N, Laverghettam A V and Lei W 2003 Differential morphology of pyramidal tract-type and intratelencephalically projecting-type corticostriatal neurons and their intrastriatal terminals in rat *J. Comp. Neurol.* **457** 420–40
[35] Plonsey R and Heppner D B 1967 Considerations of quasi-stationarity in electrophysiological systems *Bull. Math. Biophys.* **29** 657–64
[36] Grant P F and Lowery M M 2009 Electric field distribution in a finite-volume head model of deep brain stimulation *Med. Eng. Phys.* **31** 1095–103
[37] International Commission of Radiological Protection 1975 *Report of the Task Group on Reference Man* vol 23 (London: Pergamon)
[38] Scheufler O, Kania N M, Heinrichs C M and Exner K 2003 Hyperplasia of the subcutaneous adipose tissue is the primary histopathologic abnormality in lipedematous scalp *Am. J. Dermatopathol.* **25** 248–52
[39] Gabriel S, Lau R W and Gabriel C 1996 The dielectric properties of biological tissues: III. Parametric models for the dielectric spectrum of tissues *Phys. Med. Biol.* **41** 2271–93
[40] Baumann S B, Wozny D R, Kelly S K and Meno F M 1997 The electrical conductivity of human cerebrospinal fluid at body temperature *IEEE Trans. Biomed. Eng.* **44** 220–3
[41] Ranck J B and BeMent S L 1965 The specific impedance of the dorsal columns of the cat: an anisotropic medium *Exp. Neurol.* **11** 451–63
[42] Nowak L G and Bullier J 1998 Axons, but not cell bodies, are activated by electrical stimulation in cortical gray matter I. Evidence from chronaxie measurements *Exp. Brain Res.* **118** 477–88
[43] Nowak L G and Bullier J 1998 Axons, but not cell bodies, are activated by electrical stimulation in cortical gray matter: II. Evidence from selective inactivation of cell

bodies and axon initial segments *Exp. Brain Res.* **118** 489–500
[44] McNeal D R 1976 Analysis of a model for excitation of myelinated nerve *IEEE Trans. Biomed. Eng.* **BME-23** 329–37
[45] Richardson A G, McIntyre C C and Grill W M 2000 Modeling the effects of electric fields on nerve fibres: influence of the myelin sheath *Med. Biol. Eng. Comput.* 07-2000 **38** 438–46
[46] Schwarz J R, Reid G and Bostock H 1995 Action potentials and membrane currents in the human node of Ranvier *Pflugers Arch.* **430** 283–92
[47] Foster K R, Bidinger J M and Carpenter D O 1976 The electrical resistivity of cytoplasm *Biophys. J.* **16** 991–1001
[48] Wesselink W A, Holsheimer J and Boom H B K 1999 A model of the electrical behaviour of myelinated sensory nerve fibres based on human data *Med. Biol. Eng. Comput.* **37** 228–35
[49] Huxley A F and Stämpfli R 1949 Evidence for saltatory conduction in peripheral myelinated nerve fibers *J. Physiol.* **108** 315–39
[50] Lei W, Jiao Y, Del Mar N and Reiner A 2004 Evidence for differential cortical input to direct pathway versus indirect pathway striatal projection neurons in rats *J. Neurosci.* **24** 8289–99
[51] Sloper J J and Powell T P S 1979 A study of the axon initial segment and proximal axon of neurons in the primate motor and somatic sensory cortices *Phil. Trans. R. Soc. Lond.* B *Bio. Sci.* **285** 173–97
[52] Lefaucheur J P, Holsheimer J, Goujon C, Keravel Y and Nguyen J 2010 Descending volleys generated by efficacious epidural motor cortex stimulation in patients with chronic neuropathic pain *Exp. Neurol.* **223** 609–14
[53] McIntyre C C and Hahn P J 2010 Network perspectives on the mechanisms of deep brain stimulation *Neurobiol. Dis.* **38** 329–37
[54] Fahn S and Elton R L 1987 *Recent Developments in Parkinson's Disease* ed S Fahn and C D Marsden *et al* (New York: Macmillan) pp 153–64
[55] Zwartjes D G M, Heida T, van Vugt J P, Geelen J A and Veltink P H 2010 Ambulatory monitoring of activities and motor symptoms in Parkinson's disease *IEEE Trans. Biomed. Eng.* **57** 2778–86
[56] Holsheimer J, Nguyen J, Lefaucheur J P and Manola L 2007 Cathodal, anodal or bifocal stimulation of the motor cortex in the management of chronic pain? *Acta Neurochir.* **S97** 57–66